



**HAL**  
open science

## Spatiotemporal dynamics of calcium signals during neutrophil cluster formation

Roxana Khazen, Béatrice Corre, Zacarias Garcia, Fabrice Lemaître, Sophie Bachellier-Bassi, Christophe D'Enfert, Philippe Bousso

► **To cite this version:**

Roxana Khazen, Béatrice Corre, Zacarias Garcia, Fabrice Lemaître, Sophie Bachellier-Bassi, et al.. Spatiotemporal dynamics of calcium signals during neutrophil cluster formation. Proceedings of the National Academy of Sciences of the United States of America, 2022, 119 (29), pp.e22038551. 10.1073/pnas.2203855119 . pasteur-03775237

**HAL Id: pasteur-03775237**

**<https://pasteur.hal.science/pasteur-03775237>**

Submitted on 12 Sep 2022

**HAL** is a multi-disciplinary open access archive for the deposit and dissemination of scientific research documents, whether they are published or not. The documents may come from teaching and research institutions in France or abroad, or from public or private research centers.

L'archive ouverte pluridisciplinaire **HAL**, est destinée au dépôt et à la diffusion de documents scientifiques de niveau recherche, publiés ou non, émanant des établissements d'enseignement et de recherche français ou étrangers, des laboratoires publics ou privés.



Distributed under a Creative Commons Attribution - NoDerivatives 4.0 International License

**Spatiotemporal dynamics of calcium signals  
during neutrophil cluster formation**

Roxana Khazen<sup>1</sup>, Béatrice Corre<sup>1</sup>, Zacarias Garcia<sup>1</sup>, Fabrice Lemaître<sup>1</sup>

Sophie Bachellier-Bassi<sup>2</sup>, Christophe d'Enfert<sup>2</sup> and Philippe Bousso<sup>1</sup>

<sup>1</sup> Dynamics of Immune Responses Unit, Institut Pasteur, Université de Paris, INSERM U1223, Paris, France.

<sup>2</sup> Unité Biologie et Pathogénicité Fongiques, Institut Pasteur, Université de Paris, INRAE, USC2019, Paris, France.

Correspondence to [philippe.bousso@pasteur.fr](mailto:philippe.bousso@pasteur.fr)

**Neutrophils form cellular clusters or swarms in response to injury or pathogen intrusion. Yet, intracellular signaling events favoring this coordinated response remain to be fully characterized. Here, we show that calcium signals play a critical role during mouse neutrophils clustering around particles of zymosan, a structural fungal component. Pioneer neutrophils recognizing zymosan or live *Candida albicans* displayed elevated calcium levels. Subsequently, a transient wave of calcium signals in neighboring cells was observed followed by the attraction of neutrophils that exhibited more persistent calcium signals as they reached zymosan particles. Calcium signals promoted LTB4 production while blocking of extracellular calcium entry or LTB4 signaling abrogated cluster formation. Finally, using optogenetics to manipulate calcium influx in primary neutrophils, we show that calcium signals could initiate recruitment of neighboring neutrophils in an LTB4 dependent-manner. Thus, sustained calcium responses at the center of the cluster is necessary and sufficient for the generation of chemoattractive gradients that attract neutrophils in a self-reinforcing process.**

**Significance Statement:** During tissue damage or infection, neutrophils rapidly engage into a coordinated migration to form clusters. Neutrophil clustering is believed to contribute to wound sealing or pathogen clearance. Here we investigate the signals responsible for this collective behavior. We found that calcium signals in neutrophils recognizing microbial products promote the production the neutrophil attractant LTB4, favoring the migration of additional neutrophils toward the cluster and additional calcium signals in a self-amplifying phenomenon.

## Introduction

Neutrophils represent an essential and rapid line of defense against a variety of pathogens. One hallmark of neutrophil behavior *in vivo* is their ability to form clusters or swarms in response to injury or infection (1-6). This phenomenon ensures the clearance of localized pathogens and promotes the sealing of tissue wounds but may also have deleterious effects such as alteration of lymph node architecture (1) or the formation of skin abscess (7). Such neutrophil collective behavior has been initially uncovered with the help of intravital imaging (1, 2, 4). Additionally, *in vitro* methods have been developed to study neutrophil clusters with high throughput (8). During neutrophil cluster formation, one or a few pioneer neutrophils (3) reach the site of damage/infection followed within minutes by the rapid and directional migration of many additional neutrophils toward the cluster (9). At later time points, neutrophil aggregation stops and mechanisms promoting cluster termination include chemoattractant receptor desensitization (10, 11) and factors secreted in the late phase of neutrophil aggregation such as LXA<sub>4</sub> (8). Central to this type of coordinated behavior is neutrophil ability to produce and respond to the same chemoattractants, forming the basis for a self-amplifying phenomenon (4, 8, 12). In a variety of settings, Leukotriene B<sub>4</sub> (LTB<sub>4</sub>) has been shown to be a major chemoattractant driving neutrophil cluster formation (4, 8, 9, 12).

Despite a detailed understanding of the spatiotemporal dynamics of neutrophil cluster formation, several key questions remain unanswered. Which signal drives pioneer neutrophil activity? In the context of sterile injury, cell death events have been shown to play an essential role in neutrophil swarming (4, 13). Whether neutrophil clusters during infection also primarily rely on cell death events or can be initiated by specific intracellular signaling events is unclear. Moreover, how neutrophils communicate in order to achieve spatially organized chemoattractant production remains to be fully understood. In an elegant study, Sarris and

colleagues demonstrated that, in the context of sterile injury in zebrafish larvae, neutrophils communicate using ATP through connexin hemichannel to generate calcium signals and produce LTB<sub>4</sub> within the cluster (14). Whether calcium signals are also involved during mammalian neutrophil clustering and recognition of microbial products has not been investigated. It is also unclear whether calcium signals are sufficient to promote neutrophil clustering.

Here, we investigate the role of calcium signals in mouse neutrophil clusters formed during recognition of the fungal product, zymosan. Using *in vitro* and *in vivo* imaging, we show that zymosan recognition by pioneer neutrophil elicit a strong calcium response and transient calcium response in neighboring neutrophils that subsequently migrated directionally toward the cluster. Upon reaching zymosan particle, attracted neutrophils exhibited a sustained calcium elevation concomitant with their arrest. We provide evidence that LTB<sub>4</sub> production and calcium signaling were required for cluster amplification. Finally, by manipulating calcium signals by optogenetics, we show that calcium elevation is by itself sufficient to initiate some aspects of neutrophil clustering. Thus, spatially organized calcium signals orchestrate the self-amplifying neutrophil attraction that leads to cluster formation.

## Results

### **Zymosan induced neutrophil clusters *in vivo***

To model neutrophil cluster formation upon recognition of microbial products, we used zymosan, a component of fungal cell wall. Zymosan particles have been previously shown to trigger neutrophil clustering *in vitro* (8). To test whether zymosan could also induce neutrophil clusters *in vivo*, we injected fluorescent zymosan particles in the ear of LysM-eGFP mice (in which neutrophils express high levels of GFP) and performed intravital imaging. Neutrophils displayed strong accumulation and attraction toward the zymosan spot (**Figure 1A-B, Movie 1**). Migrating neutrophils arrested when reaching the zymosan particles (**Movie 1**). In contrast, no clusters were detected in zymosan-free areas (**Figure 1A-B, Movie 1**). Thus, zymosan effectively induced neutrophil clustering *in vivo*. Neutrophil swarms were not only detected in response to zymosan particles but were also detected following injection of live *Candida albicans in vivo* (**Fig 1C, Movie 2**).

### **Calcium signals during neutrophil cluster formation *in vitro***

Next, we thought to determine the initial signals triggering neutrophil cluster formation. Recognition of zymosan by neutrophils or macrophages can induce  $\text{Ca}^{2+}$  influx (15, 16). When performing live imaging of neutrophil recognition of single zymosan particles *in vitro*, we observed that neutrophils increased intracellular calcium and arrested upon contact with zymosan (**Figure 2A-B, Movie 3**). Additional calcium peaks were seen after the particles had been phagocytized (**Movie 3**). To investigate the spatiotemporal dynamics of calcium signals during neutrophil cluster formation, we imaged Indo1-loaded neutrophils in the presence of zymosan spots (containing 15-30 particles) as multiple zymosan particles are needed to elicit neutrophil clusters (8). We could identify several stages during neutrophil cluster formation

(**Figure 2C, Movie 4**). The first step consisted in one or a few neutrophils interacting with zymosan particles. These pioneer neutrophils exhibited strong calcium elevation and were completely arrested (**Movie 4**). Within a few minutes, a wave of transient calcium signal propagated from the nascent cluster to all neutrophils present within a radius of 100-150  $\mu\text{m}$  from the center of the cluster (**Figure 2C-D, Movie 4**). Upon rapid return of intracellular calcium concentration to basal levels, most neutrophils in this ‘alert’ zone changed morphology, becoming more elongated and starting to migrate directionally toward the cluster (**Figure 2E-G, Movie 4**). As these neutrophils were approaching the cluster, they exhibited sporadic calcium responses that became prolonged as they joined the pool of neutrophils contacting the zymosan particles (**Figure 2G-I, Movie 4**). A collective and sustained calcium elevation at the center of the cluster was typically detected for the remaining duration of the movie (1h). These results indicated that zymosan-induced neutrophil clusters are associated with robust calcium responses prominent at the center of the cluster and extending to more distant neutrophils (up to 100-150  $\mu\text{m}$  away) in a more transient manner. Notably, neutrophil recognition of live *Candida albicans* also resulted in calcium responses associated with cluster formation (**Figure S1, Movie 5**). Since loss of membrane integrity can lead to intracellular calcium elevation, we tested whether some of the detected calcium signals were due to cell death events. However, repeating these experiments in the presence of propidium iodide did not support a major role for cell death in the signals detected (**Figure 2J, Movie 6**).

To test the importance of calcium influx in the process of neutrophil clustering, we analyzed neutrophils in the presence of zymosan and EGTA in order to chelate extracellular calcium. Neutrophil cluster formation was abrogated in the absence of extracellular calcium, suggesting that calcium influx is required for the coordinated neutrophil clustering (**Figure 3, Movie 7**). We also tested the impact of calcium chelation at later time point when the cluster had already started to form. As shown in **Movie 8**, addition of EGTA rapidly arrested ongoing neutrophil

cluster formation. It remains formally possible that calcium chelation affects other aspects of neutrophil biology such as adhesion properties that could potentially limit cluster formation. However, blocking CD18 did not prevent cluster formation around zymosan particles (Figure S2). Our results supported the idea that calcium signals play a major role during neutrophil cluster formation in these *in vitro* settings.

### **Robust calcium signaling during neutrophil clustering *in vivo***

To test whether calcium signals are also associated with cluster formation *in vivo*, we generated bone marrow chimeras by reconstitution of irradiated mice with hematopoietic stem cells (HSC) retrovirally transduced to express the genetically-encoded calcium reporter, Twitch2B (17) (**Figure 4A-B**). Chimeric mice were injected with zymosan particles in the ear dermis and immediately subjected to intravital imaging. As expected, cells with the typical morphology and migratory behavior of neutrophils rapidly accumulated around the zymosan spot once pioneer cells reached the zymosan particles (**Figure 4C-D, Movie 9**). Clusters were not detected in areas without zymosan (**Figure 4C**). Most importantly, we observed strong and prolonged calcium elevation in neutrophils contacting the zymosan while approaching neutrophils exhibited transient calcium responses (**Movie 9**). Thus, neutrophil cluster formation is also associated with strong calcium signaling *in vivo*.

### **Reciprocal amplification of calcium signals and LTB<sub>4</sub> production participate in neutrophil clustering**

We next asked how calcium signals at sites of zymosan recognition may contribute to cluster formation. The lipid mediator LTB<sub>4</sub> is well known to participate in neutrophil swarming in response to sterile injury or pathogens. Zymosan recognition by neutrophils induced LTB<sub>4</sub> production that was largely dependent on extracellular calcium (**Figure 5A-B**). Moreover,

eliciting a calcium influx in neutrophils using thapsigargin directly triggered LTB<sub>4</sub> production (**Figure 5A-B**). Reciprocally, neutrophils exhibited increased intracellular calcium concentration in response to LTB<sub>4</sub> (**Figure 5C**). Moreover, antagonizing LTB<sub>4</sub> receptors largely reduced neutrophil clustering around zymosan particles (**Figure 5D-E, Movie 10**). In these settings, the early calcium wave was reduced and subsequent calcium signals were only detected in neutrophils initially contacting the zymosan particles (**Movie 10**). No attraction of remote neutrophils was observed. To confirm the importance of LTB<sub>4</sub> in our settings, we used MK886 an inhibitor of Arachidonate 5-Lipoxygenase (Alox5), an essential enzyme for LTB<sub>4</sub> synthesis. As shown in **Figure 5F-G**, neutrophils strongly reduced cluster formation around zymosan in the presence of MK886. We also tested the role of connexin hemichannels as well as ATP production since they play an important role in neutrophil swarming in zebrafish model of sterile injury. Cluster formation was not affected in the presence of NF279, an antagonist of P2X receptors (**Figure 5F-G**). In the presence of Carbenoxole (CBX), an inhibitor of gap-junctions, neutrophils also continued to form large clusters around zymosan particles with a modest reduction in cluster size that did not reach statistical significance (**Figure 5F-G**). This suggest that propagation of calcium signals through ATP and connexins is dispensable for neutrophils clustering triggered by zymosan recognition.

Our results support a model in which zymosan recognition directly triggers calcium elevation and LTB<sub>4</sub> production, attracting more neutrophils that engage in LTB<sub>4</sub> production as they approach and reach the zymosan spot (responding to local LTB<sub>4</sub> concentration and zymosan particles).

### **Optogenetic manipulation of calcium signals in neutrophils supports a causative role for calcium in cluster formation**

Our results and that of a recent study (14) support a role for calcium signals during neutrophil clustering in mouse and zebrafish, respectively. However, it is unclear whether calcium signals are by themselves sufficient to initiate some aspects of neutrophil cluster. To address this issue, we relied on optogenetics to directly manipulate neutrophils with light. We used the eOS1 actuator, an improved version of OptoSTIM1, that relies on Cry2-mediated clustering of STIM-1 upon light exposure to trigger calcium release-activated calcium (CRAC) channel opening and extracellular calcium influx (18). To introduce the actuator in primary neutrophils, we generated bone marrow chimeras by retroviral transduction of eOS1 in HSCs (**Figure 6A-B**). After reconstitution, neutrophils were purified from chimeric mice. We confirmed that eOS1 positive but not eOS1 negative neutrophils exhibited intracellular calcium elevation upon blue light illumination as detected by flow cytometry (**Figure 6C**). Using live imaging, we also photoactivated a mixture of neutrophils from eOS1 chimeras and control mice. As shown in **Figure 6D**, only eOS1 positive but not control neutrophils responded to a short light pulse. To test whether calcium influx in individual neutrophils may recapitulate some aspects of neutrophil clustering, we illuminated neutrophils from the chimeric mice (containing approximately 30% of eOS1 positive neutrophils). We observed that after photoactivation, isolated responding neutrophils could promote the attraction and calcium responses of neighboring neutrophils (**Figure 6E, Movie 11**), whereas no cluster were induced when control neutrophils (that did not express eOS1) were photoactivated (**Figure 6E**). Of note, only small clusters were formed possibly because additional factors (not associated with calcium signals) were missing or because only isolated cells were stimulated (as opposed to multiple cells in a zymosan spot). To confirm that neutrophil aggregates generated by optogenetic manipulation of calcium signals also shared the requirement for LTB<sub>4</sub> signaling, we performed photoactivation in the presence of BLT1/BLT2 antagonists. As shown in **Figure 6F-G**, both the number of clusters formed and the size of the clusters were substantially reduced when

interfering with LTB4 signaling. In summary, our optogenetic manipulation strongly suggested that calcium signals have a causative contribution to LTB4-dependent neutrophil cluster formation.

## Discussion

We characterized here the spatiotemporal dynamics of calcium signals during neutrophil clustering (or swarming) around the fungal component zymosan *in vitro* and *in vivo*. Calcium signals appeared spatially organized, being prominent at the cluster center and essential to promote the self-amplification phenomenon mediated in part through LTB4 production and signaling. In a model of sterile injury in the zebrafish, neutrophils were recently shown to exhibit strong intracluster calcium responses, favored by the recognition of necrotic tissue and intercellular neutrophil communication through ATP and connexin-43 hemichannels (14). In our settings, direct recognition of zymosan particles appears sufficient to elicit calcium signals in neutrophils. This is consistent with the fact that zymosan recognition by Dectin-1 triggers a calcium flux in neutrophils that is dependent on Stim1 and Stim2 (16). Such strong signaling event may also bypass the need cell death of pioneer neutrophils to initiate clustering as seen in models of tissue damage (19, 20). Thus, while signals triggering calcium elevation may vary in distinct contexts and likely coexist, an intense calcium response at the cluster center may represent a general feature of LTB4-mediated neutrophil attraction. Moreover, such a local chemoattractant production is further favored by the fact that intracellular calcium elevation promotes cell arrest (21-23) and hence cell accumulation over time. Calcium signals were both necessary and to some extent sufficient for cluster formation. Yet, it was notable that optogenetic manipulation in isolated neutrophils lead to the formation of cluster of small sizes,

in line with the proposed idea that a quorum sensing mechanism controls neutrophil cluster formation (24). Future *in vivo* application of optogenetics in neutrophils may help understand how the number of stimulated neutrophils control the size and duration of cellular clusters and whether forcing neutrophil clustering may have beneficial consequences in the context of infection or cancer. In sum, neutrophils can use recognition of microbial products and calcium signals to amplify their own recruitment in a spatially organized manner. Uncovering the tissue distribution of chemoattractants over time remains a challenging goal but could provide additional key insights into the complex process of neutrophil clustering *in vivo*.

## **Acknowledgements**

We thank members of the Bousso laboratory and M. Sarris for critical review of the manuscript.

We thank CB\_UTechS at Institut Pasteur for support in conducting the present study. The work was supported by Institut Pasteur, INSERM and an advanced grant (ENLIGHTEN) from the European Research Council. R.K. was supported by fellowships from the Cancerpole and Fondation ARC.

## **Author contributions**

R.K., B.C., F.L. and Z.G. conducted the experiments. R.K. and P.B. designed the experiments. C.E and S.B-R provided important reagents. R.K, B.C. and P.B. analyzed the data and R.K. and P.B. wrote the manuscript.

## **Conflict of interest**

The authors have no conflict of interest to declare.

## Figure legends

### **Figure 1. Zymosan and live *Candida albicans* trigger neutrophil cluster formation *in vivo*.**

LysM-eGFP mice were injected in the ear with zymosan particles and subjected to two-photon imaging for 1 hour. (A) Representative time-lapse images showing that neutrophils (green) form a large cluster around zymosan particles (lower panel) but do not cluster in area without zymosan (upper panel). (B) Accumulation of neutrophils was quantified in the indicated regions (dashed circle) by measuring GFP fluorescence intensity over time. Values were normalized over the initial mean intensity measured at time zero. Scale bar, 50  $\mu\text{m}$ . Representative of 3 independent experiments. (C) Neutrophil clustering in response to live *Candida albicans*. LysM-eGFP mice were injected in the ear with live GFP-expressing *Candida albicans* and subjected to two-photon imaging for up to 2 hours. Representative time-lapse images showing that neutrophils (green) form a cellular clusters around *Candida albicans*. Neutrophils and *C. albicans* both expressed GFP but were discriminated on the basis of their fluorescence intensity.

### **Figure 2. Spatiotemporal dynamics of calcium signals during neutrophil clustering**

Neutrophils were labeled with the calcium indicator Indo-1 and cultured with zymosan particles. (A) Representative time-lapse images showing that recognition of zymosan particles by single neutrophils (white arrows) induces calcium signaling. Scale bar, 10  $\mu\text{m}$ . Images are representative of 3 independent experiments. (B) Calcium index is graphed over time for an additional example of neutrophil contacting a zymosan particle and for a neutrophil that do not interact with zymosan. Black arrow on magenta curve indicates the time of contact between the neutrophil and the zymosan particle. (C) Calcium dynamics during neutrophil clustering proceed in different stages. Time lapse images showing different stages of neutrophil cluster

formation over a spot of zymosan particles. Yellow dashed lines delineate zoomed in areas shown in the lower panel. Scale bar upper panel, 50  $\mu\text{m}$ , lower panel 10  $\mu\text{m}$ . Representative of 3 independent experiments. **(D)** Propagation of a transient calcium wave from the center of the zymosan spot. The area showing neutrophils with elevated calcium is quantified at the indicated time points after the initial calcium response in pioneer neutrophils. Data are representative of 3 independent experiments. Bars show means  $\pm$  SEM. Groups were compared using a two-tailed unpaired t-test, \*\*\* $p < 0.001$ , \*\* $p < 0.01$ , ns: non-significant. **(E)** Time lapse images showing the morphological changes in neutrophil shape after the transient calcium wave. White dashed lines highlight neutrophil cell shape. **(F)** Quantification of the cell sphericity index during and after the transient calcium wave. A circular shape corresponds to an index of 1. Each dot represents one neutrophil. Only cells exhibiting a calcium response were analyzed. Bars represent mean values. Statistical significance was assessed using a two-tailed unpaired t-test, \*\*\* $p < 0.001$ . **(G)** Representative tracks of neutrophils migrating toward a zymosan spot. Each line corresponds to a neutrophil trajectory. Tracks are color-coded with calcium levels, showing calcium elevation in approaching neutrophils. The white circle delineates the zymosan spot. **(H)** Percentage of neutrophils with elevated calcium content was measured at different distances from the center of zymosan particles and plotted over time. **(I)** Figure compiles calcium signals in representative neutrophils before and after reaching zymosan spot (upper panel). Each line represents one neutrophil followed over time. Data are aligned to the time of zymosan recognition. Colored squares show the time points during which the neutrophil is visible within the imaging field. Orange and green indicate the time period during which the calcium level in neutrophil is low or high, respectively. Magenta box indicates the initial time point at which neutrophils reach zymosan spot. The lower panel shows representative neutrophils that did not participate in the cluster. Data are representative of at least five independent experiments. **(J)** Neutrophil clustering was imaged in the presence of propidium

iodide (red) to detect dead cells. Scale bar, 10  $\mu\text{m}$ . Results are representative of 3 independent experiments.

**Figure 3. The formation of neutrophil clusters around zymosan particles requires extracellular calcium.**

(A) Representative time lapse images of Indo-1 labeled neutrophils cluster formation around zymosan spot in the presence (lower panel) or absence (upper panel) of 0.5mM EGTA. Scale bar, 10  $\mu\text{m}$ . (B) Quantification of neutrophil density over time in the presence (black) or absence (red) of 0.5 mM EGTA. Data are pooled from 3 independent experiments.

**Figure 4. Robust calcium signals during neutrophil clustering *in vivo*.**

(A) Experimental set-up. Chimeric mice were reconstituted with HSCs expressing the FRET-based calcium indicator Twitch2B. Eight weeks later, mice were injected with zymosan particles in the ear and subjected to intravital imaging. (B) Flow cytometry dot plots showing the reconstitution of chimeric mice and percentage of neutrophils expressing Twitch2B. (C) Time-lapse images showing calcium levels (as measured by FRET signals with Twitch2B) in neutrophils in the presence (lower panel) or absence (upper panel) of a zymosan spot (magenta). Scale bar, 50  $\mu\text{m}$ . (D) Quantification of absolute number of neutrophils clustering at zymosan spot during 2 hours of imaging. Data are pooled from 2 independent experiments. (E) Figure compiles calcium signals in several neutrophils before and after reaching zymosan spot. Each line represents one neutrophil followed over time. Data are aligned to the time of zymosan recognition. Colored squares show the time points during which the neutrophil is visible within the imaging field. Orange and green indicate the time period during which the calcium level in neutrophil is low or high, respectively. Magenta box indicates the initial time point at which neutrophils reach zymosan spot. Data are representative of 3 independent experiments.

**Figure 5. Calcium signals and LTB4 production participates jointly in neutrophil cluster formation and expansion.**

(A) Neutrophils secrete LTB4 in the presence of zymosan particles or upon treatment with thapsigargin. Statistical significance was assessed using two-tailed unpaired t-test. \*\*\* $p < 0.001$ . (B) LTB4 production by neutrophils in response to zymosan in the presence or absence of EGTA. (C) Intracellular calcium elevation in Indo-1 labeled neutrophils treated with 50ng/ml of LTB4 using time-resolved flow cytometry. Calcium responses are shown as averaged kinetic curves. (D) Time-lapse images of Indo-1 labeled neutrophils around a zymosan spot (magenta) in the presence or absence of 20 $\mu$ M U75302 and 20 $\mu$ M LY255283 (BLT1 and BLT2 antagonists respectively). Scale bar, 10  $\mu$ m. Data are pooled from 3 independent experiments. (E) Quantification of neutrophil density over time in the presence (black) or absence of 20 $\mu$ M U75302 and 20 $\mu$ M LY255283 (red). (F-G) Neutrophil cluster formation was evaluated in the presence of inhibitor of LTB4 synthesis MK886, the inhibitor of gap junction CBX or the antagonist of P2X receptors NF279. (F) Representative time-lapse images depicting neutrophil clustering in the presence or absence of the indicated drug. (G) Quantification of neutrophil cluster size around zymosan particles normalized to number of zymosan particles per spot. Statistical significance was assessed using two-tailed unpaired t-test. \*\*\* $p < 0.001$ , ns: not significant.

**Figure 6. Optogenetic manipulation of calcium signals in neutrophils support a causative role for calcium in cluster formation.**

(A) Experimental set-up. Chimeric mice reconstituted with HSCs expressing the calcium actuator eOS1. After 8 weeks, eOS1-expressing neutrophils were isolated from the chimeras. (B) Flow cytometry dot plots showing the reconstitution of chimeric mice and percentage of

neutrophils expressing eOS1. **(C)** Neutrophils isolated from the chimeric mice were loaded with the Indo-1 calcium indicator. Cells were subjected to time-resolved flow cytometry and illuminated with an external LED (470 nm) during the acquisition at the indicated time point. Calcium responses shown as averaged kinetic curves of neutrophils expressing different levels of eOS1 plasmid (bright, dim or neg). PA indicates the timing of photoactivation during the experiment. Representative of four independent experiments. **(D)** A mixture (1:1 ratio) of neutrophils isolated from eOS1<sup>+</sup> chimeric mice (uncolored) and neutrophils isolated from wild type mice (loaded with SNARF) was prepared. Cells were loaded with Indo-1 and subjected to live imaging. Photoactivation was induced using LED (470 nm) every 10 min for 10 sec. Percentages of responding cells are shown upon each PA cycle. **(E)** Time-lapse images depicting neutrophils and calcium dynamics upon photoactivation. Arrowheads show the initial neutrophils responding to photoactivation. Dashed lines in the third and fourth panels highlight the transient Ca<sup>2+</sup> wave and the formation of a neutrophil cluster, respectively. Scale bar, 10  $\mu$ m. Data are representative of 4 independent experiments. **(F-G)** The number of formed clusters in the field of view (F) and the total number of attracted cells per cluster (G) was quantified after PA of eOS1-expressing neutrophils in the presence or absence of BLT1 and BLT2 antagonists. Data are pooled from 3 independent experiments. Bars show means  $\pm$  SEM. Groups were compared using a two-tailed unpaired t-test, \*\*p < 0.01, \*p < 0.1.

## Materials and Methods

### Mice

Six to eight week-old C57BL/6J mice were purchased from ENVIGO. LysM-eGFP mice were bred in our animal facility under specific pathogen-free conditions. We used age- and sex-matched mice for all experiments. All animal studies were approved by the Institut Pasteur Safety Committee in accordance with French and European guidelines (CETEA 190148).

### Neutrophil isolation

Femurs and tibias were isolated from adult WT or chimeric mice, sterilized in 70% ethanol and flushed with PBS. Single cell suspensions were prepared by filtering the marrow through a 70  $\mu$ m cell strainer. Neutrophils were sorted by negative selection using the mouse isolation kit following manufacture instructions (Miltenyi). Cells were then cultured in complete RPMI medium 1640 (supplemented with 10% heat-inactivated fetal bovine serum, 100 U/mL penicillin, 100 ng/mL streptomycin, 1 mM sodium pyruvate, 10 mM HEPES and 5  $\mu$ M 2-mercaptoethanol) and used within 24 hours.

### In vitro imaging of neutrophil cluster formation

Plastic dishes were coated with Poly-D-Lysine (Sigma, 0.01% dilution in H<sub>2</sub>O) for 10 min at 37°C and washed with PBS before loading cells. Neutrophils were stained with Indo-1/AM (2.5  $\mu$ M, Molecular Probes) for 40 min at 37 °C. Labeled neutrophils were washed and resuspended in complete RPMI without phenol red. Cluster formation was initiated by gently transferring labeled neutrophils in plastic dishes and adding zymosan particles (Thermofisher) at the beginning of the recording. Alternatively, zymosan particles or live GFP-expressing *Candida albicans* were pre-coated on glass dishes using micropatterning stamps (4Dcell)

following manufacturer's instructions. The fluorescent strain of *Candida albicans* (CEC4950) is a derivative of the reference strain SC5314, in which the GFP placed under the control of the strong constitutive promoter PTDH3 was integrated at the RPS1 locus. Imaging was performed using a two-photon microscope. Excitation was provided by an Insight deep see Dual laser (Spectra-Physics) tuned at 720 nm (for Indo-1, zymosan and PI imaging), 880 nm for GFP and 1040 nm (for SNARF imaging). The following filter sets were used: Indo-1: 483/32 and 390/40, PI: 624/40, zymosan-Alexa594: 593/35, SNARF: 607/70, GFP: 512/25. Temperature was maintained at 37°C with a heating ring. Ca<sup>2+</sup> signals were quantified using the ratio of calcium bound to calcium free fluorescence as described previously (18). Images were analyzed using Fiji software. Cluster formation was evaluated by measuring neutrophil density around the zymosan spot over time. For optogenetic experiments, eOS1-expressing or control neutrophils were placed in a Poly-D-Lysine-coated plate and photoactivated using a 470 nm blue light LED (Leica) for 15s. Image acquisition was performed as described above. When indicated control neutrophils were labeled with SNARF. For inhibition of BLT1 and BLT2, we used LY255283 and U75302 (dissolved in ethanol at 1mM, Abcam). Both compounds were added to the culture media at a concentration of 20 µM. Neutrophils were left in the incubator for 15 min before addition to the zymosan-coated plastic dishes. For testing the effect of EGTA on neutrophil migration during clustering, neutrophils were re-suspended in culture media containing 0.5 µM EGTA. Alternatively, EGTA was added at the same concentration 5 minutes after neutrophil cluster formation was detected.

### **Generation of bone marrow chimeric mice**

Hemopoietic cells were isolated from femurs and tibias of C57BL/6J adult mice by flushing bone marrow with PBS. Red blood cells were removed through Ficoll-Paque separation (GEHealthcare). Cells were then washed and resuspended in complete media supplemented

with 100ng of m-SCF, 20ng of m-IL-3 and 20ng of m-IL-6 (Peprotech) and incubated overnight at 37°C. These cells were retrovirally transduced to express either the FRET-based Twitch2B calcium indicator (17) or calcium actuator mScarlet-OptoSTIM-1 (eOS1) (18). Wild type C57BL/6J recipient mice were  $\gamma$ -irradiated with a single dose of 9 Gy. Four hours later, irradiated mice were reconstituted with a total of  $4 \times 10^6$  transduced bone marrow cells via i.v. injection. Mice were used 6-12 weeks after reconstitution. Reconstitution was confirmed by flow cytometry by staining blood cells with a Alexa647-conjugated anti-Ly6G-mAb (clone 1A8, BD).

### **Intravital imaging**

Mice were anesthetized with a mixture of Xylazine (Rompun®, 10 mg/kg) and Ketamine (Imalgene®, 100 mg/kg), which was replenished hourly. Zymosan-Alexa594 particles or live GFP-expressing *Candida albicans* ( $2 \times 10^4$ ) were diluted in 50 $\mu$ L PBS and 5  $\mu$ L were injected in the ear of the indicated recipients (5). Intravital imaging was performed 15 minutes after injection. Two-photon imaging was performed with an upright microscope FVMPE-RS (OLYMPUS) and a 25 $\times$ /1.05 NA water-dipping objective (OLYMPUS). Excitation was provided by an Insight deep see dual laser (Spectra Physics) tuned at 880 nm. The following filter sets were used for imaging: Twitch2B (CFP: 483/32 and YFP: 542/27), zymosan-Alexa594 (593/35), GFP (512/25). A 25- $\mu$ m-thick volume of tissue was scanned at 5- $\mu$ m Z-steps and 10 to 30s intervals. Images were processed and analyzed using Fiji software. Movies and figures based on two-photon microscopy are shown as two-dimensional maximum intensity projections of three-dimensional data.

### **Calcium measurement by flow cytometry**

Neutrophils isolated from either C57BL/6J mice or chimeric mice expressing mScarlet-eOS1 actuator were stained with Indo-1/AM (2.5  $\mu$ M, Molecular Probes) for 40 min at 37 °C. Cells were washed and kept at 37 °C in complete medium at a concentration of  $10^6$  cells/mL. Calcium measurements were performed on a CytoFLEX LX cytometer (Beckman Coulter) using CytExpert 2.3 software (Beckman Coulter). A baseline Indo-1 fluorescence was recorded for 1-2 min, cells were then photoactivated by placing a LED (470 nm, 710 mW, THORLabs) in front of the FACS tube for 60s at the indicated time point while cell acquisition continued. A calcium index was calculated as the ratio of the fluorescent signals at 405 nm ( $\text{Ca}^{2+}$  bound dye, 405/30 BP) to that at 485 nm ( $\text{Ca}^{2+}$  free dye, 525/40 BP), and followed over time. A kinetic analysis was performed with FlowJo software version 10.4 (Tree Star) and the smoothed geometric means of Indo-1 ratio were plotted.

### **Measurement of LTB4 production**

Neutrophils were resuspended in complete RPMI either untreated or stimulated with  $2 \times 10^4$  zymosan particles for 15 and 30 minutes. Alternatively, neutrophils were stimulated with a mixture of PMA (100 ng/mL) and ionomycin (1  $\mu$ g/mL) or thapsigargin (1  $\mu$ M) for 30 minutes (All purchased from Sigma). Supernatants were recovered and the secretion of LTB4 was measured using a LTB4 parameter assay kit (R&D systems).

### **Statistical analysis**

All statistical tests were performed with Prism v8 (GraphPad). Unpaired t-tests were used as indicated.

## References

1. T. Chtanova *et al.*, Dynamics of neutrophil migration in lymph nodes during infection. *Immunity* **29**, 487-496 (2008).
2. B. McDonald *et al.*, Intravascular danger signals guide neutrophils to sites of sterile inflammation. *Science* **330**, 362-366 (2010).
3. L. G. Ng *et al.*, Visualizing the neutrophil response to sterile tissue injury in mouse dermis reveals a three-phase cascade of events. *J Invest Dermatol* **131**, 2058-2068 (2011).
4. T. Lammermann *et al.*, Neutrophil swarms require LTB4 and integrins at sites of cell death in vivo. *Nature* **498**, 371-375 (2013).
5. J. L. Li *et al.*, Intravital multiphoton imaging of immune responses in the mouse ear skin. *Nat Protoc* **7**, 221-234 (2012).
6. Q. Deng *et al.*, Localized bacterial infection induces systemic activation of neutrophils through Cxcr2 signaling in zebrafish. *J Leukoc Biol* **93**, 761-769 (2013).
7. J. Liese, S. H. Rooijackers, J. A. van Strijp, R. P. Novick, M. L. Dustin, Intravital two-photon microscopy of host-pathogen interactions in a mouse model of *Staphylococcus aureus* skin abscess formation. *Cell Microbiol* **15**, 891-909 (2013).
8. E. Reategui *et al.*, Microscale arrays for the profiling of start and stop signals coordinating human-neutrophil swarming. *Nat Biomed Eng* **1** (2017).
9. K. Kienle, T. Lammermann, Neutrophil swarming: an essential process of the neutrophil tissue response. *Immunol Rev* **273**, 76-93 (2016).
10. C. Coombs *et al.*, Chemokine receptor trafficking coordinates neutrophil clustering and dispersal at wounds in zebrafish. *Nat Commun* **10**, 5166 (2019).

11. K. Kienle *et al.*, Neutrophils self-limit swarming to contain bacterial growth in vivo. *Science* **372** (2021).
12. T. Nemeth, A. Mocsai, Feedback Amplification of Neutrophil Function. *Trends Immunol* **37**, 412-424 (2016).
13. P. Sagoo *et al.*, In vivo imaging of inflammasome activation reveals a subcapsular macrophage burst response that mobilizes innate and adaptive immunity. *Nat Med* **22**, 64-71 (2016).
14. H. Poplimont *et al.*, Neutrophil Swarming in Damaged Tissue Is Orchestrated by Connexins and Cooperative Calcium Alarm Signals. *Curr Biol* **30**, 2761-2776 e2767 (2020).
15. M. Girotti, J. H. Evans, D. Burke, C. C. Leslie, Cytosolic phospholipase A2 translocates to forming phagosomes during phagocytosis of zymosan in macrophages. *J Biol Chem* **279**, 19113-19121 (2004).
16. R. A. Clemens, J. Chong, D. Grimes, Y. Hu, C. A. Lowell, STIM1 and STIM2 cooperatively regulate mouse neutrophil store-operated calcium entry and cytokine production. *Blood* **130**, 1565-1577 (2017).
17. T. Thestrup *et al.*, Optimized ratiometric calcium sensors for functional in vivo imaging of neurons and T lymphocytes. *Nat Methods* **11**, 175-182 (2014).
18. A. Bohineust, Z. Garcia, B. Corre, F. Lemaitre, P. Bousso, Optogenetic manipulation of calcium signals in single T cells in vivo. *Nat Commun* **11**, 1143 (2020).
19. H. M. Isles *et al.*, Pioneer neutrophils release chromatin within in vivo swarms. *eLife* **10** (2021).
20. K. M. Glaser, M. Mihlan, T. Lammermann, Positive feedback amplification in swarming immune cell populations. *Curr Opin Cell Biol* **72**, 156-162 (2021).

21. P. A. Negulescu, T. B. Krasieva, A. Khan, H. H. Kerschbaum, M. D. Cahalan, Polarity of T cell shape, motility, and sensitivity to antigen. *Immunity* **4**, 421-430. (1996).
22. E. Donnadieu, G. Bismuth, A. Trautmann, Antigen recognition by helper T cells elicits a sequence of distinct changes of their shape and intracellular calcium. *Curr Biol* **4**, 584-595 (1994).
23. N. R. Bhakta, D. Y. Oh, R. S. Lewis, Calcium oscillations regulate thymocyte motility during positive selection in the three-dimensional thymic environment. *Nature Immunol.* **6**, 143-151 (2005).
24. M. Palomino-Segura, A. Hidalgo, Immunity: Neutrophil Quorum at the Wound. *Curr Biol* **30**, R828-R830 (2020).

## **Movie legends**

### **Movie 1. Neutrophil clustering around zymosan particles in vivo**

LysM-eGFP mice were injected in the ear with zymosan particles and subjected to two-photon imaging for 1 hour. Time-lapse movie showing that neutrophils (green) form a large cluster around zymosan particles (magenta) but do not cluster in area without zymosan.

### **Movie 2. Neutrophils clustering around live *Candida albicans* in vivo**

LysM-eGFP mice were injected in the ear with GFP-expressing *C. albicans* and subjected to two-photon imaging. Time-lapse movie showing that neutrophil clustering around a live *C. albicans*. Neutrophils and *C. albicans* both expressed GFP but were discriminated on the basis of their fluorescence intensity.

### **Movie 3. Zymosan recognition induces calcium elevation in neutrophils**

Neutrophils were labeled with the calcium indicator Indo-1 and cultured with zymosan particles. Representative time-lapse movie showing that recognition of zymosan particles by single neutrophils induces calcium signaling.

### **Movie 4. Spatiotemporal dynamics of calcium signal during neutrophil clustering**

Neutrophils were labeled with the calcium indicator Indo-1 and cultured with zymosan particles. Calcium dynamics during neutrophil clustering proceed in different stages. Time lapse movie illustrating different stages of neutrophil cluster formation over a spot of zymosan particles.

### **Movie 5. Calcium response in neutrophils clustering around live *C. albicans*.**

Neutrophils were labeled with the calcium indicator Indo-1 and cultured with GFP-expressing live *Candida albicans*. Time lapse movie illustrating the calcium response in neutrophils clustering around live *C. albicans*.

#### **Movie 6. Calcium elevation in neutrophils is not due to cell death**

Neutrophils were labeled with the calcium indicator Indo-1 and cultured with zymosan particles in the presence of propidium iodide. Time lapse movie showing minimal cell death during neutrophil cluster formation.

#### **Movie 7. Calcium signals are required for neutrophil clustering**

Neutrophils were labeled with the calcium indicator Indo-1 and cultured with zymosan particles in the presence or absence of EGTA to chelate extracellular calcium. Representative time lapse movie showing the EGTA abrogated neutrophil cluster formation.

#### **Movie 8. Calcium signals are required during neutrophil clustering**

Neutrophils expressing the Twitch2B calcium reporter were cultured with zymosan particles. As neutrophil started to migrate toward the nascent neutrophil cluster, EGTA was added while imaging continued. Time-lapse movie showing that EGTA treatment rapidly interrupted the directed migration of neutrophils toward the cluster.

#### **Movie 9. Imaging calcium signals during neutrophil cluster formation in vivo**

Chimeric mice were reconstituted with HSCs expressing the FRET-based calcium indicator Twitch2B. Eight weeks later, mice were injected with zymosan particles in the ear and subjected to intravital imaging. Time-lapse movie showing calcium levels (as measured by FRET signals with Twitch2B) in neutrophils in the presence or absence of a zymosan spot

(magenta). The movie compiles several continuous imaging acquisitions over a period of 2 hours (acquisitions were subjected to short interruptions for focal drift corrections).

**Movie 10. LTB<sub>4</sub> play a major role in neutrophil clustering around zymosan particles**

Time-lapse movie of Indo-1 labeled neutrophils around a zymosan spot in the presence or absence of 20 $\mu$ M U75302 and 20 $\mu$ M LY255283 (BLT1 and BLT2 antagonists respectively).

**Movie 11. Optogenetic manipulation of calcium signals in neutrophils**

Chimeric mice reconstituted with HSCs expressing the calcium actuator eOS1. After 8 weeks, neutrophils were isolated from the chimeras. Neutrophils were loaded with Indo-1 and subjected to live imaging. Time-lapse movies depicting neutrophil and calcium dynamics upon photoactivation (470nm).

**Figure1**

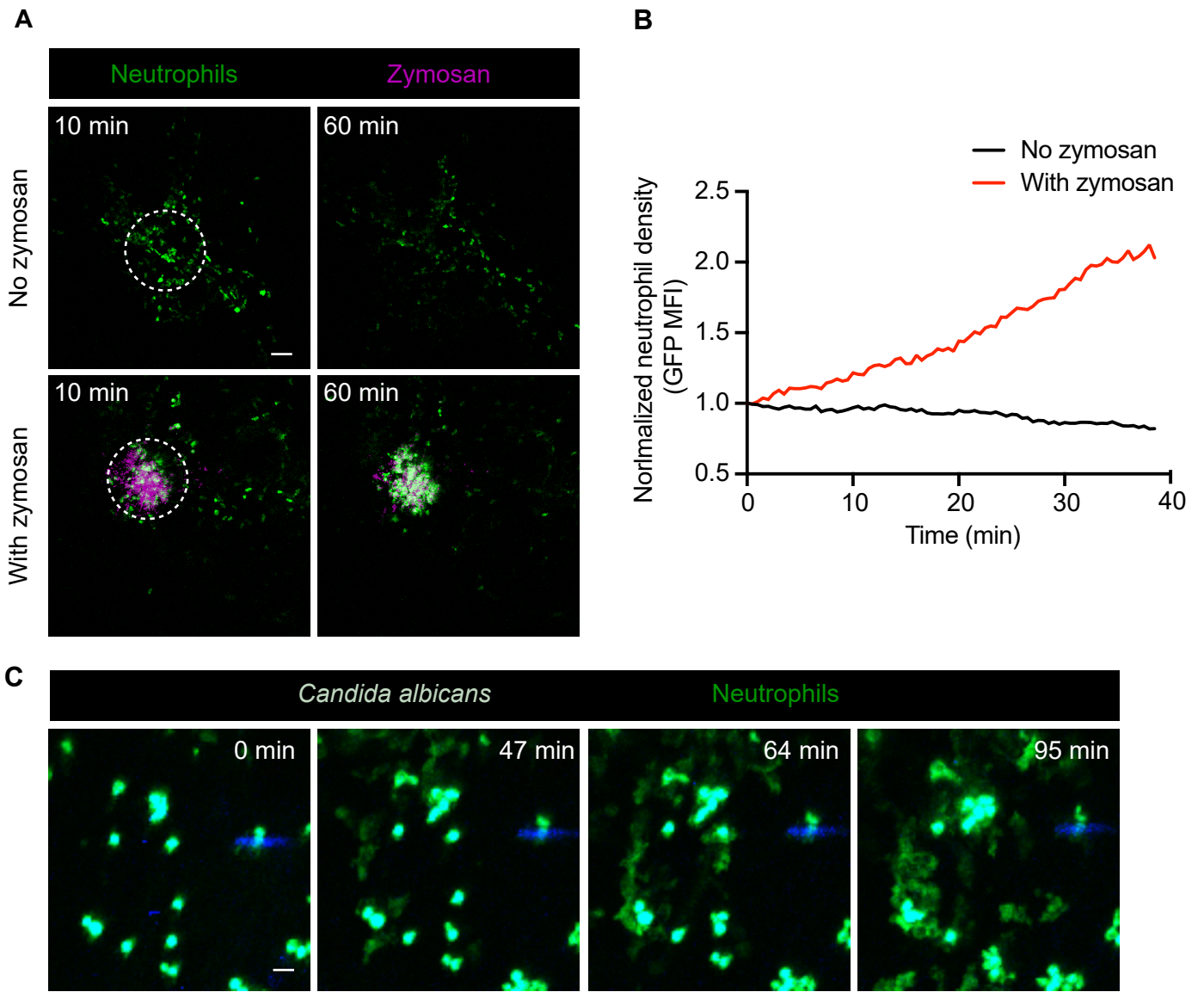


**Figure 2**

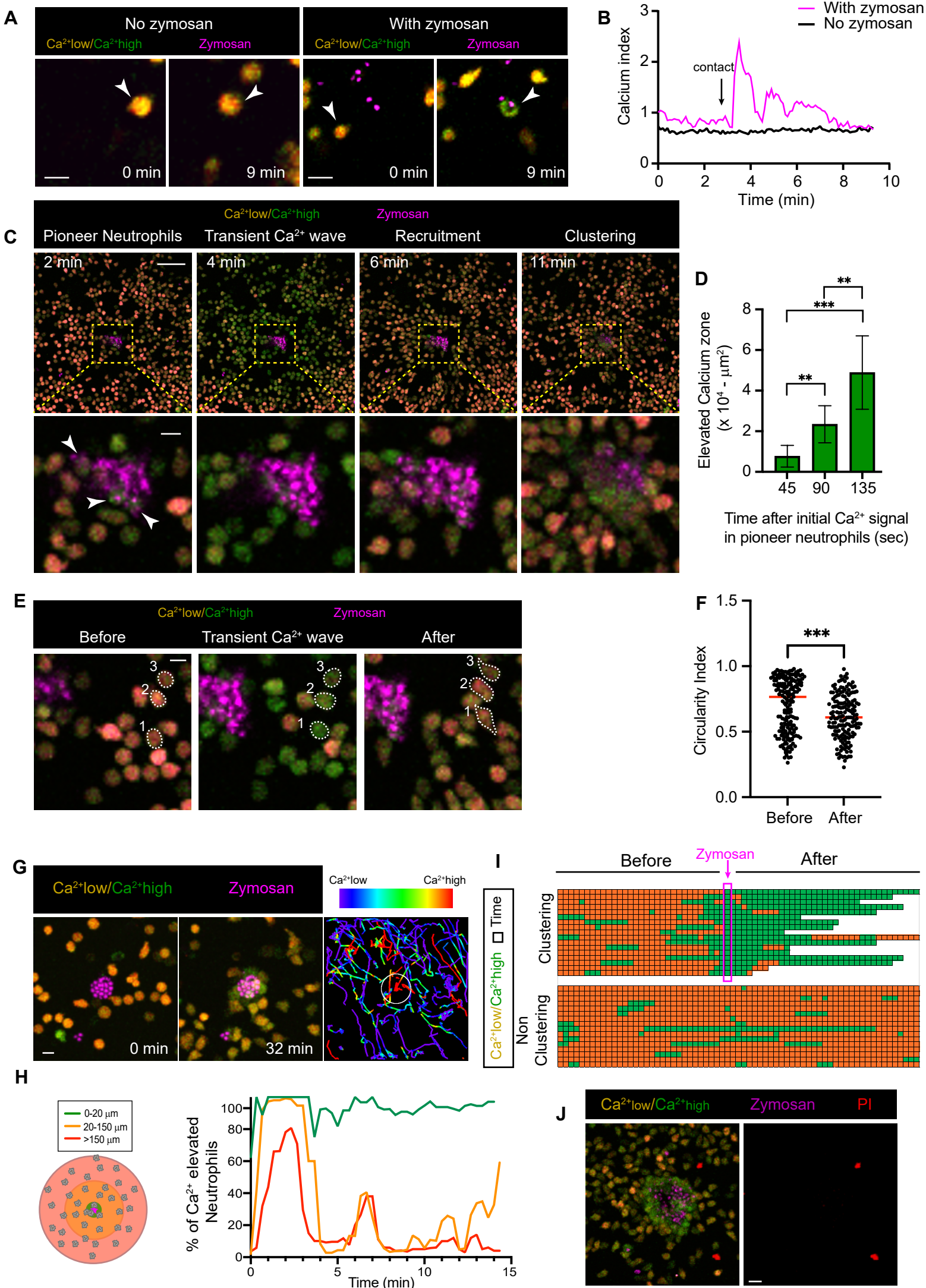
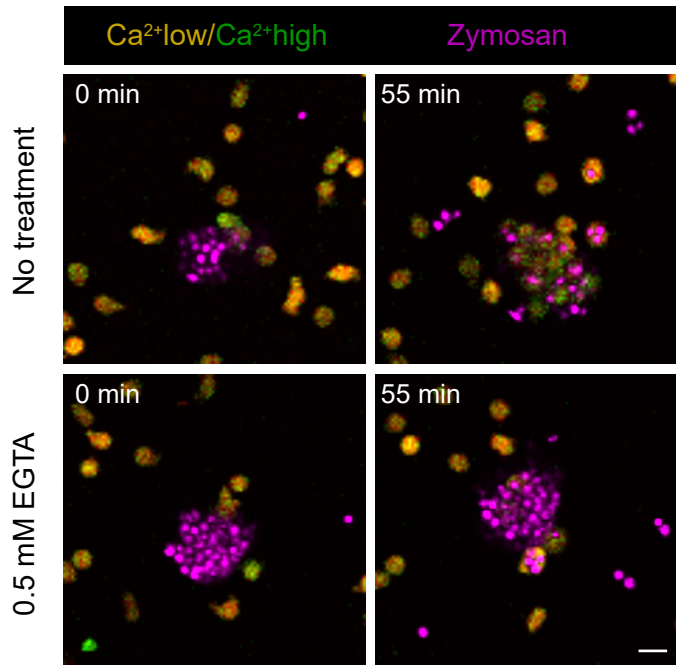
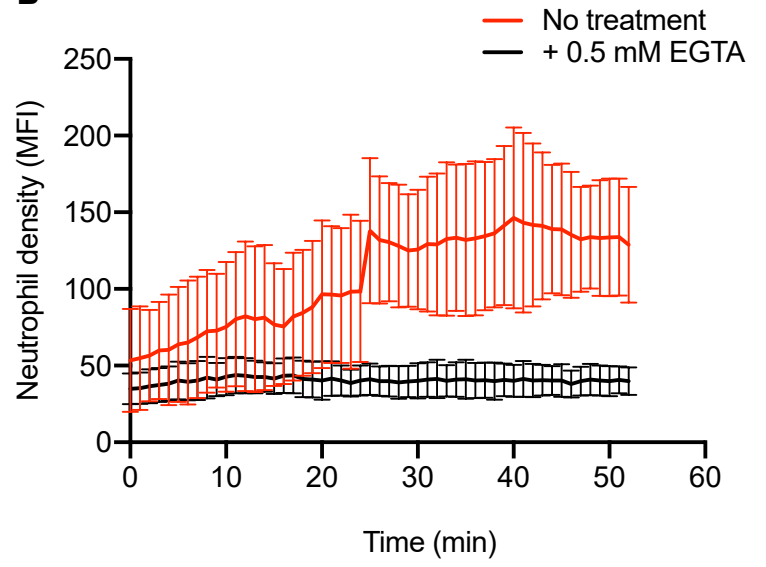


**Figure 3**

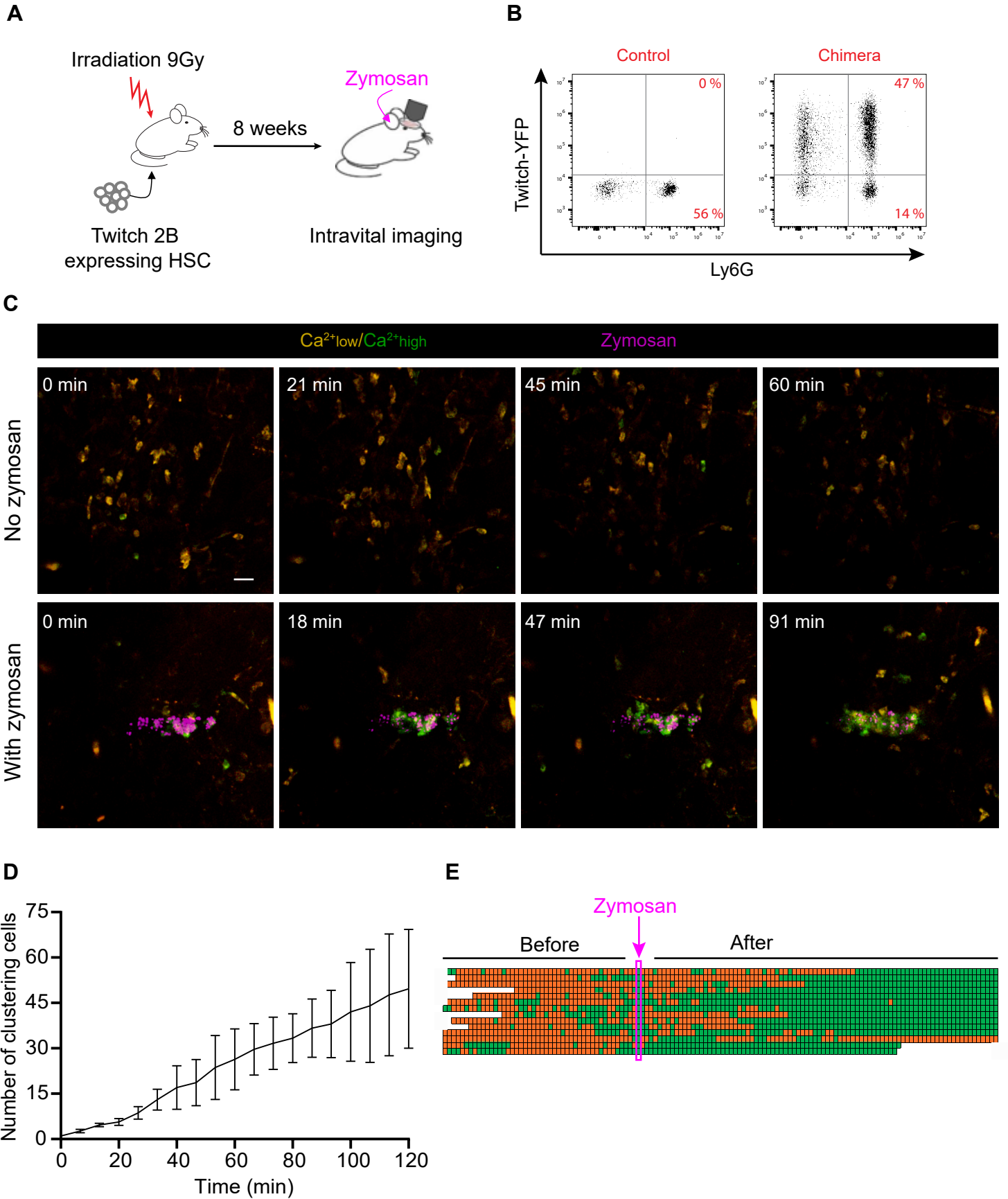
**A**

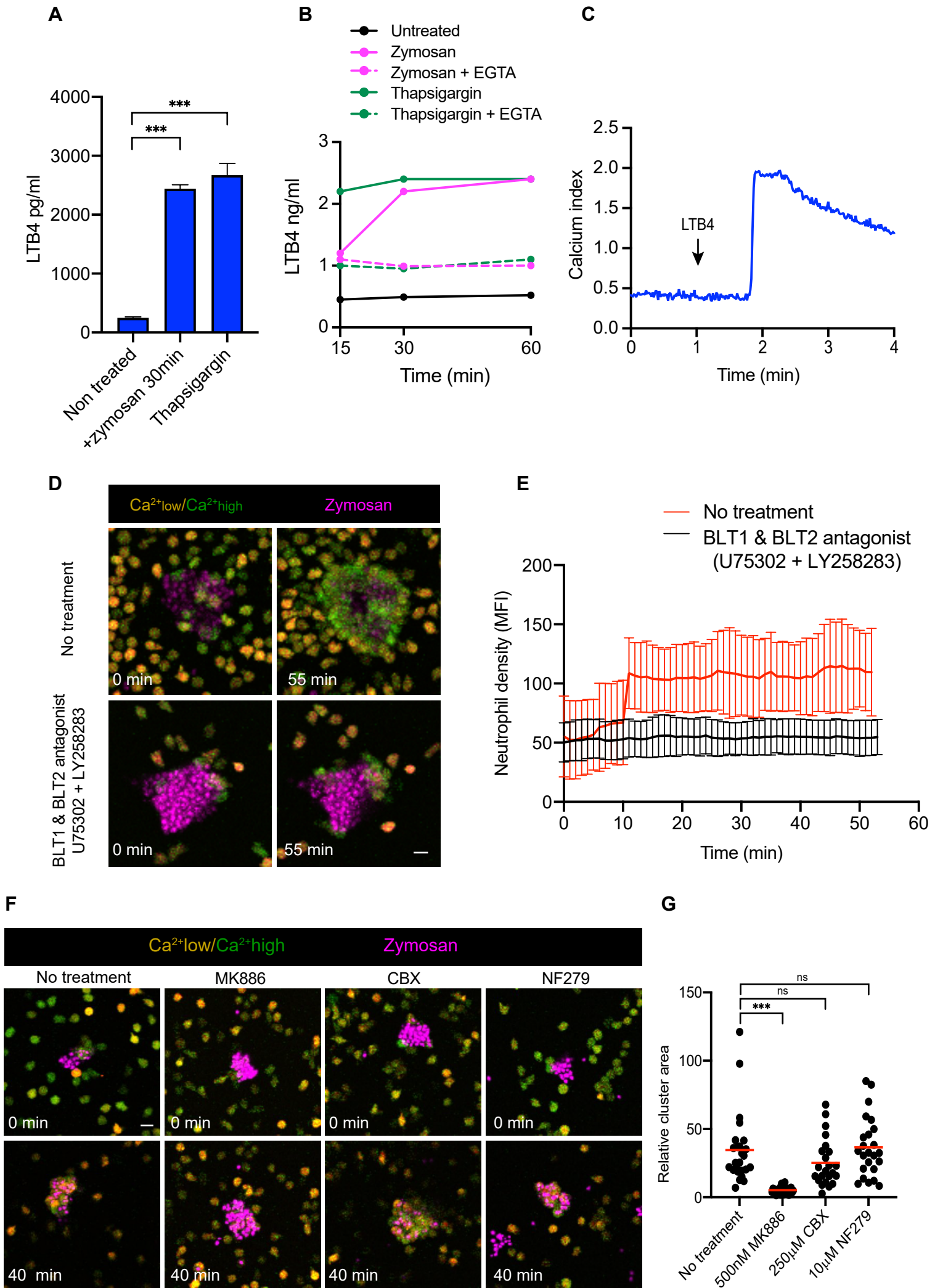


**B**



**Figure 4**



**Figure 5**

**Figure 6**